Bioconjugate Chemistry

Article

pubs.acs.org/bc

Specific Binding of Modified ZD6474 (Vandetanib) Monomer and Its Dimer with VEGF Receptor-2

Yoo-shin Kim, Feng Li, Brian E. O'Neill,* and Zheng Li*

Department of Translational Imaging, Houston Methodist Research Institute, Weill Medical College of Cornell University, 6670 Bertner Avenue, Houston, Texas 77030, United States

ABSTRACT: Tumor angiogenesis is an important component of cancer biology driven in part by the hypothesis that tumor vessel growth is a necessary requirement for tumor growth. Angiogenesis does not only depend on endothelial cell invasion and proliferation, it also requires pericyte coverage of vascular sprouts for vessel stabilization. These processes are coordinated by vascular endothelial growth factor (VEGF). Vandetanib, also known as ZD6474, is an orally bioavailable small molecule tyrosine kinase inhibitor of multiple growth factors that is an antagonist of the vascular endothelial growth factor receptor-2 (VEGFR-2). ZD6474 was purchased and modified to add a fluorescent dye (6-FAM). A linker was used to couple the ZD6474 monomer to create dimers, and similarly linked to FAM fluorescent dye. The two compounds were compared using human endothelial cell (HUVECs) and the cancer cell lines U-87-MG and MDA-MB-231. We compared cellular uptake and binding specificity, as well as effects on cellular viability and angiogenesis in a series of *in vitro* and *in vivo* studies. ZD6474 dimer demonstrated improved uptake in HUVECs and other VEGFR expressing cells over ZD6474 monomer *in vitro*. Therapeutic effects were mixed, with *in vitro* studies showing the dimer having the same or weaker effects compared to the monomer, while an *in vivo* study using pseudotumors (matrigel plug assay) seemed to indicate stronger effects could be obtained from the dimer. Finally, in biodistribution study in a xenograft tumor model, the dimer accumulated 20× greater concentration in the tumor than in the liver, spleen, or kidneys, and also 20× greater than the accumulation of the monomer or the dye alone, all at 24 h following compound injection. This study provides a rationale for the evaluation of dimeric ZD6474 as a potent imaging agent of angiogenic activity *in vivo*.

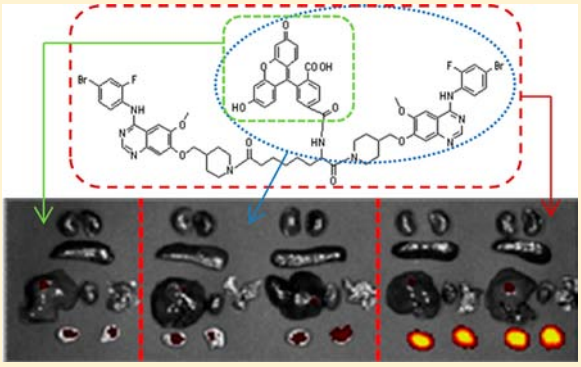

INTRODUCTION

Angiogenesis, the formation of new blood vessels from existing vasculature, is an important component of normal physiological growth and a fundamental process for tumor growth and metastasis.[1] Angiogenesis has been established as a crucial target for cancer treatment, as the process of new blood vessel formation is required to supply the oxygen and nutrients needed for tumor growth once the tumor reaches a certain size.[2,3] Angiogenic microvascular endothelial cells are a convenient target for therapeutic intervention since they are easily accessible.[4,5] Angiogenesis is a multistep process that involves endothelial cell activation, migration, proliferation, the proteolytic degradation of the extracellular matrix and the formation of capillary vessels. To trigger this process, tumor cells release a number of angiogenic growth factors such as vascular endothelial growth factor (VEGF), fibroblast growth factor basic (bFGF), and scatter factors.[6−8] Many angiogenic proteins, which are potential targets for pharmacological inhibitory strategies, depend on the inhibition of neovascularization for their biological functions. Several types of angiogenic agents are found on the cell surface and in the extracellular matrix, where they play a central role in growth factor regulation. Angiogenesis not only depends on endothelial cell (EC) invasion and proliferation, but also requires pericyte coverage of vascular sprouts for vessel stabilization.[9,10] These processes are coordinated by Vascular Endothelial Growth Factor (VEGF) and other growth factors (*b*FGF, PDGF, EGF, IGF, etc.) through their cognate receptors on ECs and vascular smooth muscle cells (VSMCs), respectively.[11−13]

VEGF, which was identified in the 1980s, is recognized as an essential regulator and a key factor of normal and abnormal blood vessel growth. In 1993, it was shown that a monoclonal antibody that targeted VEGF resulted in a dramatic suppression of tumor growth *in vivo*, which led to the development of bevacizumab (Avastin; Genentech), a humanized variant of this anti-VEGF antibody, as an anticancer agent. The recent approval of bevacizumab by the U.S. FDA as a first-line therapy for metastatic colorectal cancer validates the idea that VEGF is a key mediator of tumor angiogenesis and that blocking angiogenesis is an effective strategy to treat and detect human cancer.[14] VEGF activates endothelial cells by signaling through two high affinity receptors, the FMS-like tyrosine kinase receptor, FLT-1, and the kinase-insert domain-containing receptor, KDR.[15] In the family of VEGF receptors,

Received: August 7, 2013
Revised: September 11, 2013
Published: October 4, 2013

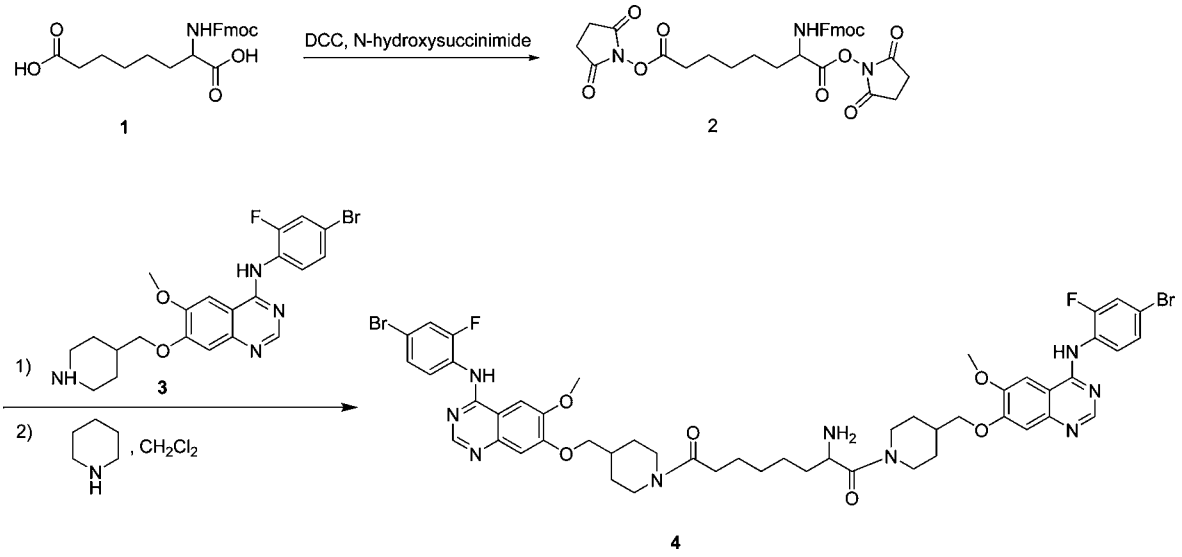

Figure 1. Schematic chemical structure of ZD6474 monomer modification and synthetic scheme of ZD6474 dimer.

VEGFR-1 is required for the recruitment of hematopoietic precursors and migration of monocytes and macrophages, whereas VEGFR-2 and VEGFR-3 are essential for the functions of vascular endothelial and lymphendothelial cells, respectively.[16] The recognition of the key role that VEGF plays in tumor angiogenesis has led to the development of various strategies to inhibit and detect VEGF signaling. Such strategies include antisense oligonucleotides, antibodies, or receptor tyrosine kinase inhibitors.[17−20] Of these approaches, the small molecule receptor tyrosine kinase inhibitors are particularly attractive. They are orally available antagonists of vascular endothelial growth factor (VEGF) receptor-2 (VEGFR-2), epidermal growth factor receptors (EGFR or HER1 or ErbB1), and RET kinase. ZD6474 (Vandetanib; Caprelsa or ZACTIMA, AstraZeneca Pharmaceuticals LP, Wilmington DE) is a lead compound in this class that is now FDA approved for the treatment of metastatic medullary thyroid cancer (MTC). ZD6474 is a once-daily, orally bioavailable anticancer drug that inhibits VEGFR-tyrosine kinase, epidermal growth factor (EGF) and RET (rearranged during transfection) receptor tyrosine kinase signaling.[21] Therefore, ZD6474, in addition to inhibiting endothelial cell proliferation through the blockade of VEGF-induced signaling, can be used to suppress tumor cell growth more directly through the blockade of EGFR autocrine signaling.[22] The antitumor effects of ZD6474 have been demonstrated *in vivo* in a wide range of preclinical models including lung, prostate, breast, ovarian, or vulval tumors.[22−25] Moreover, ZD6474 also has the potential to inhibit metastasis by prevention of primary tumor dissemination, as well as by inhibiting the growth of metastatic foci.[26,27] ZD6474 has been evaluated in over 50 clinical trials of different tumor types and is currently in phase II development for biliary, breast, and prostate cancer treatment. In this study, our focus is to use a multivalent strategy to develop new and efficient VEGFR targeted agents from ZD6474. This strategy was tested by comparing the uptake and therapeutic effects of 6-carboxyfluorescein (FAM)-conjugated ZD6474 monomer and dimer in various cell lines and *ex vivo* biodistribution study.

MATERIALS AND METHODS

General. All solvents and reagents were purchased from commercial sources and used without further purification. ^{1}H NMR was obtained on a Bruker Ultrashield at 600 MHz. Chemical shifts were reported in ppm (δ) downfield of tetramethylsilane. The purification of the crude product was carried out on a semipreparative reversed-phase high-performance liquid chromatography (HPLC) system equipped with a diode array UV−vis absorbance detector (Agilent 1200 HPLC system). Mass spectral data were recorded on a ThermoFinnigan LCQ Fleet using electrospray as the ionization method.

ZD6474 (Vandetanib) Dimer Synthesis. Dimeric ligand **4** was synthesized in three steps. (Figure 1). To the solution of compound **1**, 2-(((9*H*-fluoren-9-yl)methoxy) carbonylamino) octanedioic acid (110 mg, 0.26 mmol) in EtOAc (20 mL), DCC (110 mg, 0.53 mmol), and *N*-hydroxysuccinimide (62 mg, 0.53 mmol) were added at 0 °C. The mixture was stirred at 0 °C for 8 h (detected by TLC). The reaction mixture was filtrated to remove white solid and the solvent was evaporated under reduced pressure to get the crude intermediate **2**. Compound **2** was dissolved in DCM (20 mL) for next step reaction without further purification. ZD6474, compound **3** (270 mg, 0.53 mmol), and DIPEA (0.2 mL) was added to the previous DCM solution of compound **2**. The reaction mixture was stirred at ambient temperature for 24 h and the solvent was evaporated under reduced pressure. Ten mL 10% piperidine DCM solution was added and the mixture was stirred at room temperature for 2 h. The purification of the crude product was carried out on a semipreparative reversed-phase high-performance liquid chromatography (HPLC) system (Agilent 1200 series). Purification was performed on a Phenomenex Luna C18 (2) column 100R (250 * 10.00 mm). The flow was 4 mL/minute, with the mobile phase starting from 70% solvent A (0.05% TFA in water) and 30% solvent B (acetonenitile) to 50% solvent A and 50% solvent B at 20 min. Compound **4** was collected, lyophilized, and stored in the dark at −20 °C until use. ^{1}H NMR (600 MHz, DMSO): 11.0 (s, active H), 8.74 (m, 2H), 8.14 (d, 2H), 8.02 (m, 2H), 7.77 (m, 2H), 7.56 (m, 4H), 7.38 (t, 2H), 4.04 (m, 10H), 3.60 (m, 1H), 3.21 (4H), 3.15 (m, 2H), 2.75 (m, 2H), 2.35 (m, 2H), 1.84 (m, 4H), 1.65 (m, 2H),

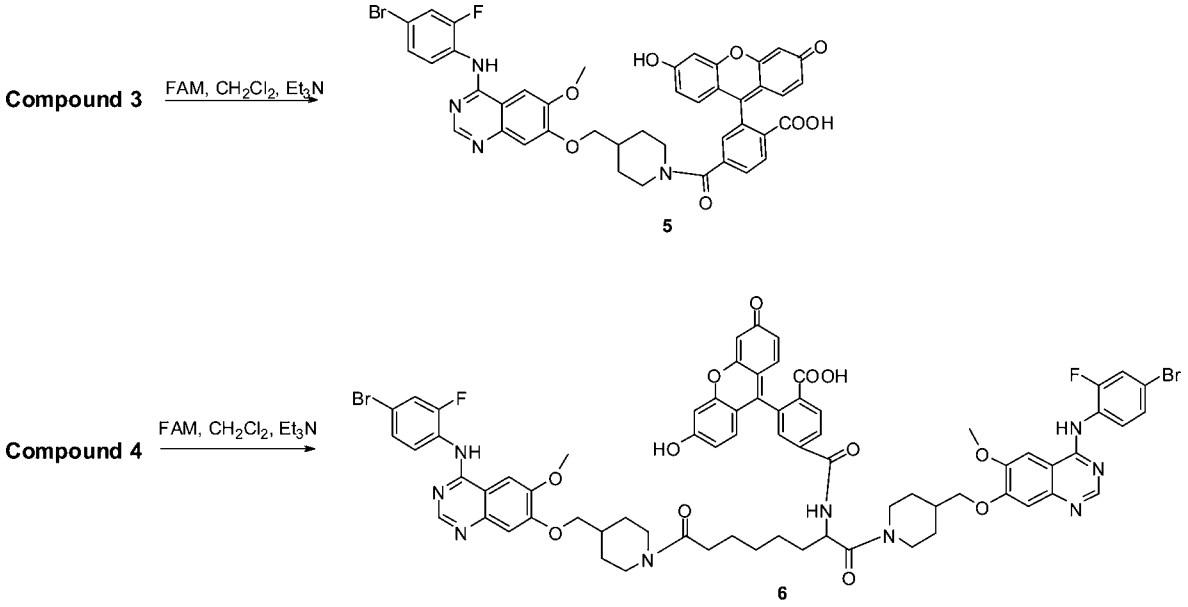

Figure 2. Synthetic scheme of 6-FAM labeled ZD6474 derivatives, monomer (**5**) and dimer (**6**).

1.43 (m, 2H), 1.18 (m, 10H). MS (electrospray): m/z 1076.6 (100, $[M+H]^+$, calcd 1075.8).

FAM-Conjugated Monomer-ZD6474 and Dimer-ZD6474 Conjugate Synthesis. The synthetic scheme of FAM conjugated compound **5** and **6** are shown in Figure 2. To a mixture of compound **3** (25 mg, 50 μmol), 6-carboxy-fluorescein succinimidyl ester (FAM, 28 mg, 60 μmol) in 3 mL DCM, 100 μL triethyl amine was slowly added. After stirring overnight in the dark at ambient temperature, the reaction was quenched by adding 200 μL of TFA. The purification of the crude product **5** was carried out on a HPLC system (Agilent 1200 series). Purification was performed on a Phenomenex Luna C18(2) column 100R (250 * 10 mm). The flow was 4 mL/minute, with the mobile phase starting from 70% solvent A (0.05 M ammonia acetate in water) and 30% solvent B (acetonenitile) to 40% solvent A and 60% solvent B at 20 min. Compound **5** was collected, lyophilized, and stored in the dark at −20 °C until use. MS (electrospray): m/z 819.2 (100, $[M+H]^+$, calcd 818.1).

Compound **6** was prepared in the similar procedure described above and purified by HPLC. Compound **6** MS (electrospray): m/z 1434.1 (100, $[M+H]^+$, calcd 1433.3). The absorption and fluorescence emission characteristics of compound **5** and **6** were identical to those of free FAM, as apparent from spectra measured in H_2O (data not shown).

***In Vitro* Cellular Uptake.** VEGFR-2 expression was established in three cell lines, MDA-MB-231 (human breast cancer cell line), U-87-MG (human glioblastoma brain cancer cell line), and HUVEC (human umbilical vascular endothelial cells). The cell lysate was separated by SDS-PAGE and transferred to nitrocellulose membranes. Membranes were probed with rabbit polyclonal antiphospho-VEGFR2 antibody (Cell Signaling Technology, Beverly, MA) followed by a goat antirabbit IgG horseradish peroxidase-conjugated secondary antibody; immunoreactive proteins were detected and visualized by chemiluminescence (ECL kit; Pierce, Rockford, IL). Proteins were separated by SDS-PAGE, and the phosphorylated proteins were probed with VEGFR-2 and antiphospho-VEGFR2. β-actin was used as a loading control.

Each of the FAM-conjugated compounds was incubated with MDA-MB-231 cells seeded 24 h earlier in a 96 well plate with 1% serum medium. Serial dilutions of the compounds were incubated for 3 h. The treated medium was then exchanged for fresh serum free medium. The remaining compound was then quantified from images taken using a Xenogen IVIS-200 (PerkinElmer, Inc. San Jose, CA) fluorescent imaging system. The same was done with HUVEC.

Blocking Assay. Specific binding of ZD6474-monomer and dimer were tested with blocking studies. Unlabeled ZD6474-monomer and ZD6474-dimer were mixed with the corresponding FAM-conjugated compounds simultaneously for 3 h. Plates were then imaged using the Xenogen IVIS-200 system. Similarly treated cells were fixed in 4% paraformaldehyde and imaged under fluorescent microscopy after staining the nuclei with DAPI.

Assay of *in Vitro* Cell Viability. MDA-MB-231 and U-87-MG cell lines were cultured in DMEM medium (Gibco, Grand Island, NY) containing 10% fetal bovine serum (FBS) and 1% penicillin streptomycin at 37 °C in a humidified atmosphere of 5% CO_2 in air. HCT 116 (human, colorectal carcinoma cell line) was grown in McCoy's 5a medium modified with 10% FBS. HUVECs (Human Umbilical Vein Endothelial cells) were grown in EGM medium (Lonza), supplemented with 20% FBS, 100 U/mL penicillin, 100 μg/mL streptomycin at 37 °C under a humidified atmosphere of 5% CO_2 and 95% O_2 with same condition as above. For the cell viability assay, the cells were then seeded into 96-well flat-bottomed tissue-culture plates at 1×10^4 cells/well and incubated for 24 or 72 h in humidified atmosphere of 5% (v/v) CO_2 at 37 °C in the presence of each compound. For HUVECs, the flat-bottomed 96-well plate (Corning, NY, USA) was coated 1 h at 37 °C with gelatin (0.3% in PBS, pH 7.4) and then washed with PBS. The cells were then treated with ZD6474 monomer and its dimer compounds in the range from 5 nM to 100 μM concentration mixed with 1% FBS added culture medium (HUVECs was 2% FBS added). Following 24 and 72 h of incubation under 5% CO_2 at 37 °C, the cells were washed with PBS and cell viability was assessed by MTT colorimetric assay. The absorbance of individual wells was measured by using an automated

dx.doi.org/10.1021/bc400374t | *Bioconjugate Chem.* 2013, 24, 1937−1944

microplate reader (570 nm; VERSAmax, Molecular Devices Corp., Sunnyvale, CA). The data are expressed as the percentage of viable cells compared to the survival of a control group and were presented as mean ± s.e. (n = 6).

***In Vitro* Tubular Formation and *in Vivo* Angiogenesis Assessment Using the Matrigel Plug Assay.** *In vitro* endothelial tube formation was performed as described in the literature.[29] Growth factor reduced Matrigel (100 μL, BD Bioscience, San Jose, CA, USA) was added to each well of a 96-well plate and allowed to polymerize for 30 min at 37 °C. HUVECs were suspended in the medium at the density of 4 × 10^5 cells per milliliter, and 0.1 mL of the cell suspension was added to each well coated with Matrigel in the presence of ZD6474 monomer or ZD6474 dimer. Cells were incubated at 37 °C for 6 h, and then photographed. The branch points were counted and averaged.

The matrigel plug assays were performed as described previously.[29] Briefly, 637 μL of growth factor reduced liquid Matrigel-PBS mixture was injected subcutaneously into the flanks of nu/nu nude mice at 4 °C. Once inside the animals, the liquid Matrigel−PBS mixture solidifies. For comparison, Matrigel alone as well as Matrigel containing $VEGF_{165}$ (Peprotech, Rocky Hill, NJ) at a final concentration of 500 ng/mL to stimulate angiogenesis, and Matrigel with $VEGF_{165}$ along with either ZD6474 monomer, ZD6474 dimer at a final concentration of 100 μM were used. All of the injection groups consisted of three mice. After 10 days, the mice were sacrificed and the Matrigel plugs were removed, fixed in 4% formalin and photographed.

***In Vivo* Animal Model and *ex Vivo* Tumor Accumulation and Biodistribution Imaging Study.** The subcutaneous dorsa of five nu/nu female mice (6 weeks old; 20 g) were inoculated bilaterally with 1 × 10^7 U87-MG human glioblastoma cells overexpressing the VEGF receptor. Once the tumor diameter was approximately 7−8 mm at 21 days post implant, the mice were divided into three groups for the following injections: (a) free FAM (n = 1), (b) FAM-labeled ZD6474-monomer (50 μM; n = 2), and (c) FAM-labeled ZD6474-dimer (50 μM, n = 2). The animals were manually restrained during intravenous tail injection. All tail vein injections were carried out with a 31 gauge needle placed in a lateral tail vein to inject 100 μL of solution. Twenty-four hours post injection, fluorescence images were acquired using a one second exposure time. The tumors and major organs were dissected and imaged again. Control (free FAM) and targeted (FAM labeled monomer and dimer) *ex vivo* tumor and organ tissue were imaged in parallel under fixed settings. *In vivo* fluorescence imaging was performed using the Xenogen IVIS 200 imaging system. To better observe the signal without losses and background due to intervening tissue, fluorescence images were collected *ex vivo*. Raw counts for each organ were measured using the Xenogen software by drawing oval regions of interest (ROI) around the organ of interest. The results were given as received photon flux per unit time in each of these ROIs, normalized by the incident light intensity. An estimate of the percentage of injected dose accumulated in the tumors was established by comparing measured counts/volume of tissue with the measured counts/volume of a known concentration of the same compound in water at the same exposure. A dilution low enough to avoid quenching was used and the results were linearly extrapolated to produce a conservative estimate of the compound concentration in the tissue. From there, the total amount of compound can be estimated and compared to the injected dose.

Statistics. The statistical significance of differences between interesting pairs of observations were determined using a two-tailed Student's t test. A two parameter linear model was applied to the tubular networks data considering interaction of compound and dose. Statistical significance was considered to be present at P values <0.05.

RESULTS

Cellular Uptake of FAM-Labeled ZD6474 Monomer and Dimer on MDA-MB-231 and HUVECS. Based on *in*

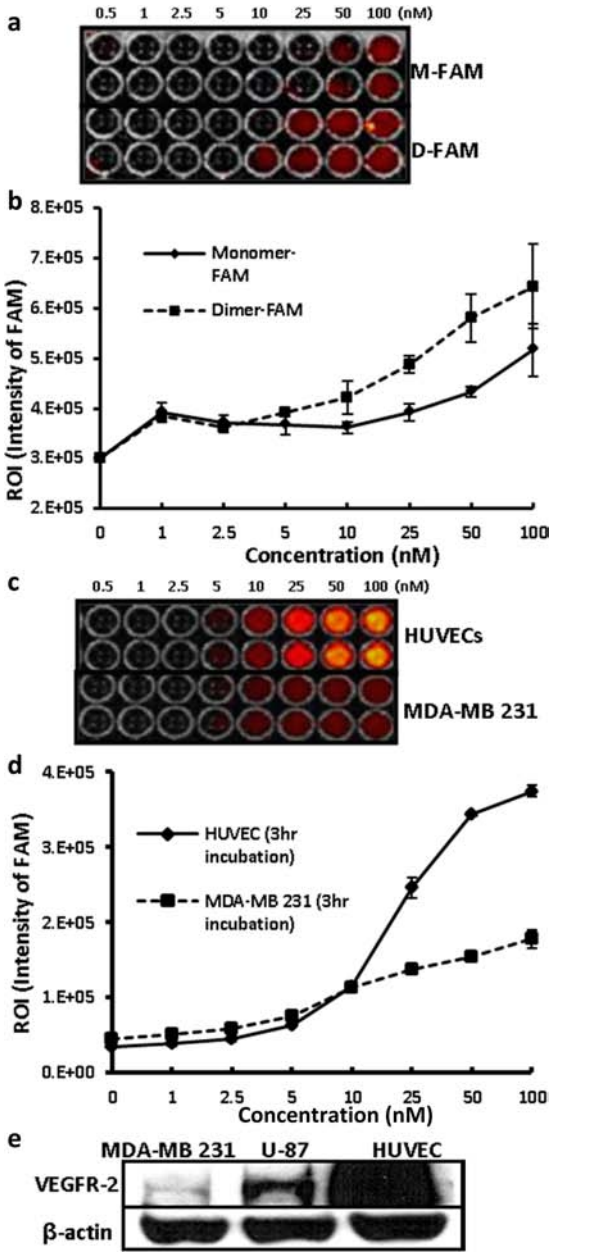

Figure 3. Fluorescence intensity of 6-FAM-conjugated ZD6474-monomer and ZD6474-dimer uptake by MDA-MB-231 cells (a) with quantification (b). Intensity comparison of 6-FAM conjugated ZD6474-dimer uptake by MDA-MB-231 cell and HUVEC cell (c) with quantification at 3 h (d). (e) Comparative expression of VEGFR-2 in three cell lines.

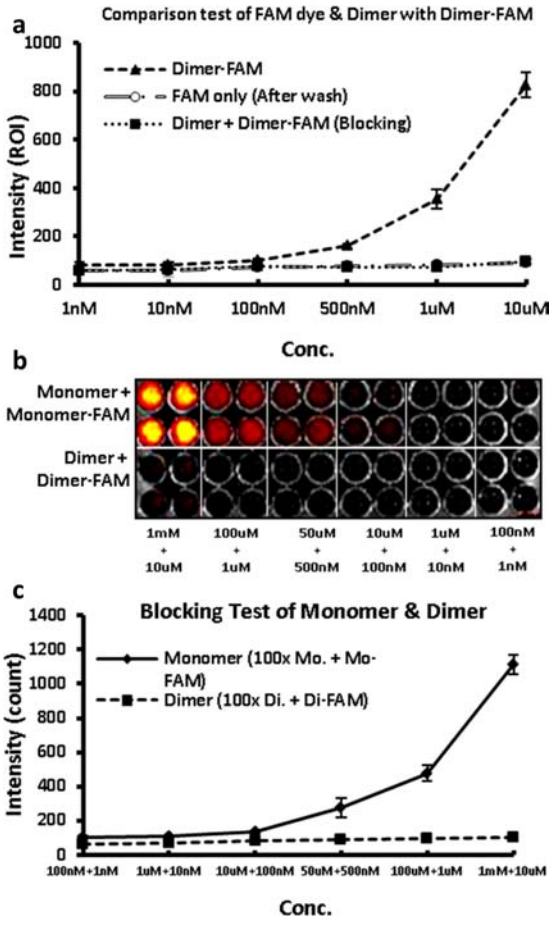

Figure 4. Blocking test on HUVEC. (a) ZD6474-dimer-FAM blocked by 100× ZD6474-dimer. (b,c) Comparison of blocking efficiency between ZD6474-monomer and ZD6474-dimer.

vitro assays, there appears to be minimal difference in uptake between monomer and dimer in the two cell lines, MDA-MB-231 and HUVECs (maximum $P = 0.09$ for 100 nM dose; Figure 3a,b). There was overall higher uptake of dimer-FAM by HUVECs rather than MDA-MB-231 cells ($P < 10^{-11}$ at 100 nM dose, Figure 3c,d), although from 1 μM to 10 μM concentration, the signal was almost the same for both cell lines (Figure 3c). Figure 3e shows comparative expression of VEGFR-2 in the three cell lines used in our studies, U-87 glioblastoma, MDA-MB-231, and HUVECs. U-87 shows higher expression compared to the MDA-MB-231 breast cancer cell line, with even more expression in the HUVEC cell line.

***In Vitro* Blocking of VEGF Receptor on HUVECs Using 6-FAM Labeled ZD6474-Dimer.** Results of the receptor blocking studies are shown in Figure 4. The decrease of signal intensity due to receptor saturation by addition of excess (100× dose) of unlabeled compound, both monomer and dimer, is shown in Figure 4b and quantified in Figure 4a,c. Figure 4a shows almost 90% loss of dimer-FAM signal when mixed with unlabeled dimer ($P < 10^{-6}$ for 10 μM dose). This is nearly identical to the signal from nonspecific binding of FAM. Figure 4c directly compares the blocking of monomer and dimer, with the dimer showing much stronger blocking and specificity. The mean signal from blocked monomer-FAM is over 10× greater than the same from dimer FAM ($P < 10^{-7}$ for 10 μM dose). The intracellular distribution of the FAM-labeled dimer is shown in Figure 5, with and without blocking via cold dimer.

***In Vitro* Cytotoxicity of Monomer and Dimer.** The cytotoxicity of ZD6474-monomer and ZD6474-dimer on cultured MDA-MB-231 (human breast cancer), HCT-116 (human colon cancer), U-87-MG (human brain glioblastoma), and HUVECS (human endothelial cells) are shown in Figure 6. Both drugs showed low toxicity to the cancer cells for a wide range of concentrations in the experimental range from 5 nM to 50 μM. Even at 100 μM, around 50% of cells treated with the monomer or dimer remained viable for the cancer cell lines (Figure 6a,b,c). In HUVECs, however, both monomer and dimer began to affect cell viability starting at the 500 nM concentration. From this dose and upward, endothelial cells are slowly dying (Figure 6d).

Inhibitory Effect of ZD6474 Derivatives on Angiogenesis *in Vitro* and *in Vivo*. Cell alignments and tubular structure formations were observed in control wells of

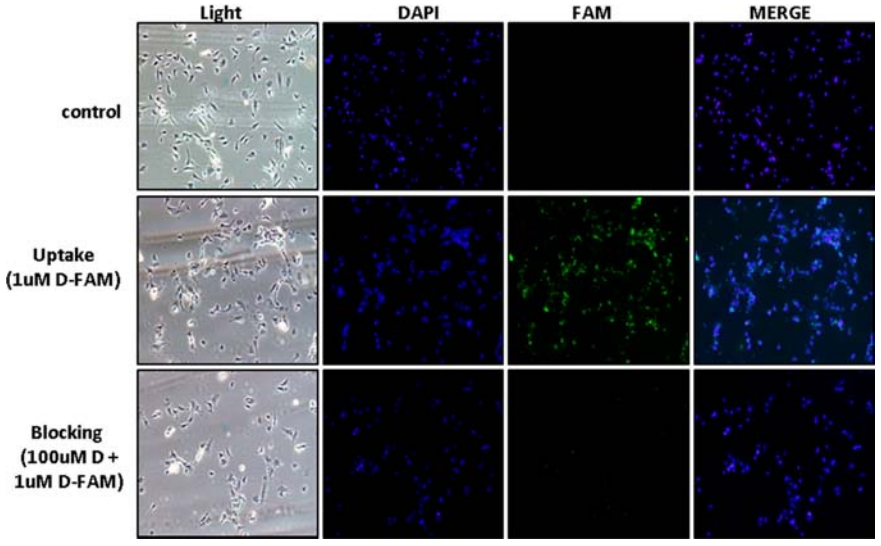

Figure 5. Cellular uptake images of HUVEC cells incubated with 1 μM FAM-conjugated ZD6474-dimer (uptake), 1 μL FAM-conjugated ZD6474-dimer and 100 μM ZD6474-dimer (blocking) and PBS (control). Complete blocking of fluorescence in blocking study demonstrated the high VEGFr specificity of the agent.

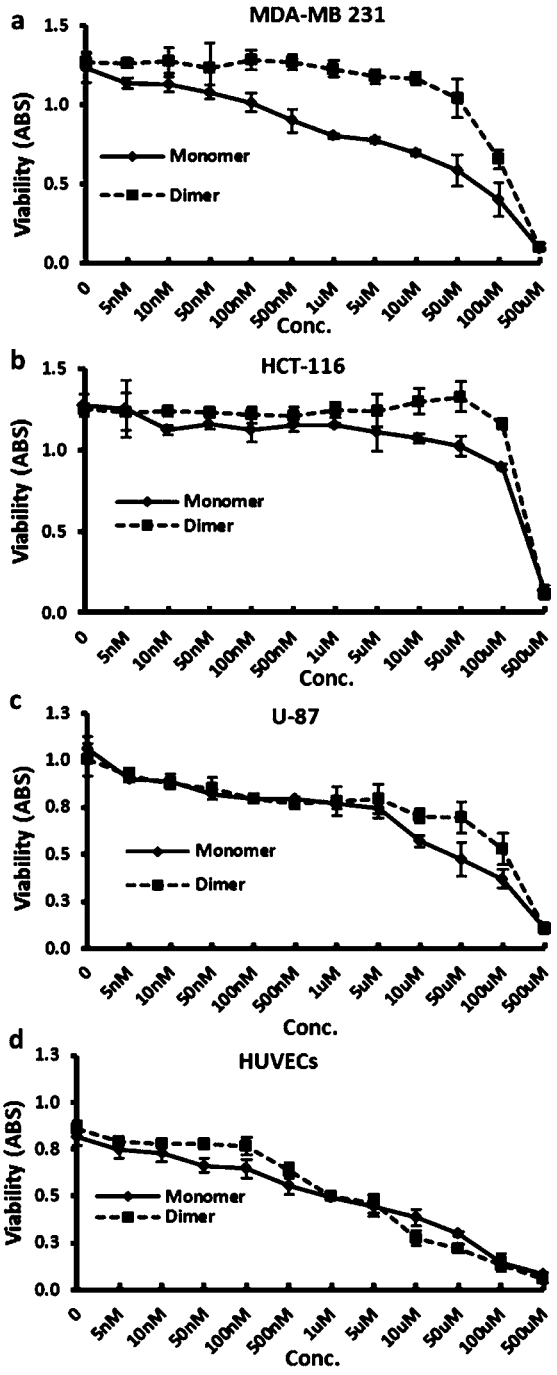

Figure 6. *In vitro* cytotoxicity ZD6474-monomer, Zd6474-dimer against MDA-MB-231, HCT-116, U-87, and HUVEC cell lines after the incubation of 72 h (a-d). The results represent the means ± SD.

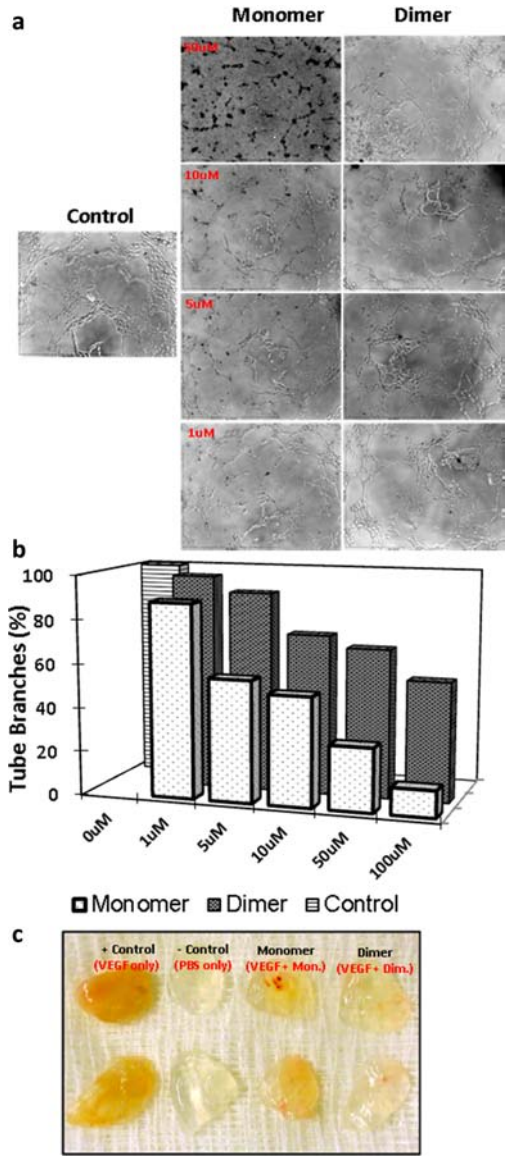

Figure 7. *In vitro* tubular formation in HUVECs (a,b) shows significant dose dependent inhibitory effect of both monomer and dimer on endothelial cell function ($P < 0.001$). The monomer is significantly stronger than the dimer ($P < 0.001$) with a stronger dose dependency ($P < 0.05$). *In vivo*, however, the dimer appears better able to inhibit the induction of angiogenesis (c).

HUVECs, as is typical of endothelial cell behavior. Cells treated with ZD6474 derivatives showed inhibitory effects (Figure 7a). ZD6474-monomer exhibited greater inhibitory effect against cell alignment and tubular structure formation than ZD6474-dimer ($P = 0.005$). Both monomer and dimer demonstrated a strong dose-dependent inhibition of tube formation ($P < 10^{-4}$), with the dose effect somewhat stronger in the monomer ($P = 0.05$). The number of tube branches was reduced from 100% in the control group to 52.0 ± 4.8% (ZD6474-monomer, 10 μM) and 75 ± 5.2% (ZD6474-dimer, 10 μM), respectively (Figure 7b). As the incubation period continued to 6 h, HUVECs treated with both ZD6474 derivatives gradually lost intercellular contact.

Figure 7c shows the *in vivo* effect on of the compounds on angiogenesis determined by the matrigel plug assay. The plugs treated with $VEGF_{165}$ alone were dark red in color, indicating the formation of new blood vessels and existing red blood cells in circulation. Negative controls showed no such color. Plugs mixed with ZD6474-monomer were paler in color than the positive controls but not entirely clear, implying significant inhibition of blood vessel development within the matrigel. On the other hand, plugs treated with ZD6474-dimer and $VEGF_{165}$ were almost the same as the PBS treated negative control group. These results imply that ZD6474-dimer was more effective in preventing microvessel formation of $VEGF_{165}$-induced angiogenesis than ZD6474-monomer *in vivo*.

dx.doi.org/10.1021/bc400374t | *Bioconjugate Chem.* 2013, 24, 1937−1944

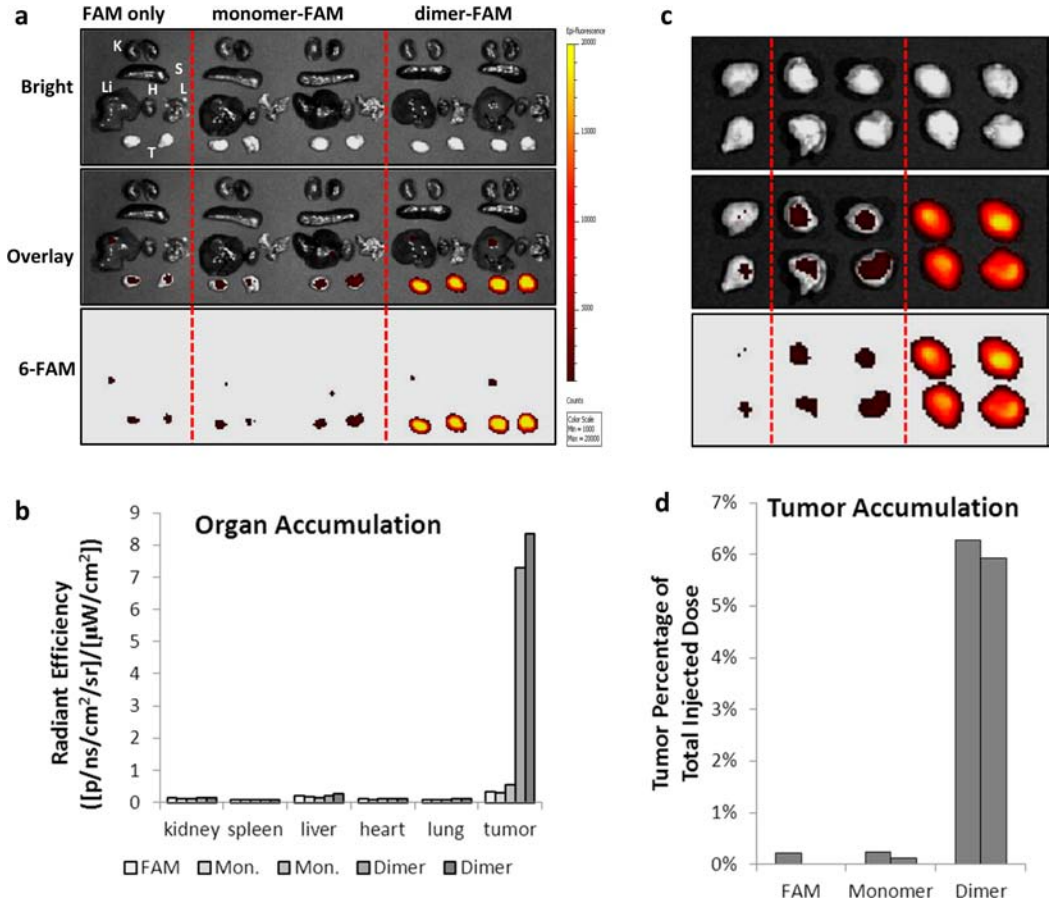

Figure 8. *Ex vivo* images of tissue distribution of FAM dye, and FAM-dye conjugated ZD6474 monomer and dimer in a bilateral U-87 tumor xenograft model in 5 animals. Images are taken and analyzed 24 h after i.v. injection of compound using a Xenogen IVIS 200 imaging box in a single exposure. Raw photon counts (a) and radiant efficiency (photon counts per unit time per unit area normalized by incident photon flux) (b) demonstrate organ distribution. Tumor and kidney values are averaged within the same animal. Close-up of tumor uptake (c) and estimated total tumor accumulation as a percent of the injected dose (d). The difference between monomer and dimer uptake is highly significant ($P < 0.001$).

***Ex Vivo* Imaging of VEGF Overexpression in Xenograft U-87 Tumor.** After the i.v. injection of 6-FAM-labeled ZD6474 derivatives in mice carrying subcutaneous xenografts of U-87 glioblastoma, the fluorescence intensity immediately increased in the whole body, due to the rapid circulation of 6-FAM-labeled ZD6474 derivatives. However, the NIR fluorescence signal in the whole body decreased as the time elapsed. The 6-FAM-labeled ZD6474-dimer displayed stronger fluorescence signals than ZD6474-monomer in the tumor regions compared to whole body. *Ex vivo* images at the 24 h time point following i.v. injection showed about 20× greater fluorescent intensity coming from the ZD6474-dimer group tumors than from tumors in other groups and from organs (Figure 8a,b). Tumor uptake of FAM dye, monomer-FAM, and dimer-FAM (Figure 8c), when compared with images of known dye concentrations, demonstrated that at least 6% of the total injected dose of the dimer-FAM ended up in the tumors compared to less than 0.25% of both FAM and monomer-FAM (Figure 8d). Despite the low sample numbers, the difference is highly significant, with $P < 0.001$ using a two-sided t test.

CONCLUSION AND DISCUSSION

In this paper, we have described a new dimeric version of an antiangiogenic drug, ZD6474, with improved cell binding and biodistribution. One would generally expect that these criteria would lead to improved therapeutic effect; however, our results on that issue are mixed. *In vitro* tests (cytotoxicity studies, tubular network formation) showed somewhat weaker cytotoxic effects against cancer and endothelial cells when compared to the monomer, while the dimer appeared to have had a stronger effect in slowing vascular invasion *in vivo* (matrigel plug assay). This apparent discrepancy may be due to differences in cultured vs natural endothelial cells or differences in pharmacokinetics or biodistributions between the two experiments. A complete resolution of this question would require a comprehensive study in animals and is beyond the scope of this paper. On the other hand, we have demonstrated that the dimer has stronger binding affinity to cells expressing the VEGF receptor (*in vitro* cellular uptake studies), better specificity (competitive binding/blocking studies), and much better tumor uptake (*in vivo* studies) than the monomer. In this last analysis, we obtained a greater than 20-fold increase in uptake in going from monomer to dimer, and showed that the dimer tumor accumulation at 24 h post injection constitutes at minimum 6% of the total injected dose. This number is a conservative estimate, in that it does not include consideration of possible quenching effects at this high concentration, nor does it account for signal losses during propagation through the tissue, neither of which effects exist in the low dose water dilution we used as a standard. The ZD6474-dimer is therefore well positioned as an imaging agent for tumor angiogenesis. Going forward, we will improve the imaging quality by

dx.doi.org/10.1021/bc400374t | *Bioconjugate Chem.* 2013, 24, 1937−1944

exchanging the 6-FAM for a near-infrared dye or a nuclear imaging moiety. We also believe that it may be possible to achieve improved therapeutic activity by conjugating to a stronger therapeutic moiety such as doxorubicin or paclitaxel.

In conclusion, we have demonstrated a dimeric version of ZD6474 with improved binding and imaging potential for angiogenic tumors compared to the original monomer.

AUTHOR INFORMATION

Corresponding Authors

*E-mail: BEOneill@HoustonMethodist.org. Tel: +1-713-441-8695.

*E-mail: ZLi@HoustonMethodist.org. Tel: +1-713-441-7962.

Notes

The authors declare no competing financial interest.

ACKNOWLEDGMENTS

The authors gratefully acknowledge the funding support of the Houston Methodist Research Institute and the intellectual contributions of Dr. King Li in supporting this project.

REFERENCES

(1) Folkman, J. (1971) Tumor angiogenesis: therapeutic implications. *N. Engl. J. Med. 285*, 1182−1186.

(2) Brem, S., Brem, H., Folkman, J., Finkelstein, D., and Patz, A. (1976) Prolonged tumor dormancy by prevention of neovascularization in the vitreous. *Cancer Res. 36*, 2807−2812.

(3) Parangi, S., Dietrich, W., Christofori, G., Lander, E. S., and Hanahan, D. (1995) Tumor suppressor loci on mouse chromosomes 9 and 16 are lost at distinct stages of tumorigenesis in a transgenic model of islet cell carcinoma. *Cancer Res. 55*, 6071−6076.

(4) Griffioen, A. W., and Molema, G. (2000) Angiogenesis: potentials for pharmacologic intervention in the treatment of cancer, cardiovascular diseases, and chronic inflammation. *Pharmacol. Rev. 52*, 237−268.

(5) Carmeliet, P., and Jain, R. K. (2000) Angiogenesis in cancer and other diseases. *Nature 407*, 249−257.

(6) Senger, D. R., Perruzzi, C. A., Feder, J., and Dvorak, H. F. (1986) A highly conserved vascular permeability factor secreted by a variety of human and rodent tumor cell lines. *Cancer Res. 46*, 5629−5632.

(7) Schmidt, N. O., Westphal, M., Hagel, C., Ergün, S., Stavrou, D., Rosen, E. M., and Lamszus, K. (1999) Levels of vascular endothelial growth factor, hepatocyte growth factor/scatter factor and basic fibroblast growth factor in human gliomas and their relation to angiogenesis. *Int. J. Cancer 84*, 10−18.

(8) Kumar, R., Kuniyasu, H., Bucana, C. D., Wilson, M. R., and Fidler, I. J. (1998) Spatial and temporal expression of angiogenic molecules during tumor growth and progression. *Oncol. Res. 10*, 301−311.

(9) Carmeliet, P. (2005) Angiogenesis in life, disease and medicine. *Nature 438*, 932−936.

(10) Andrae, J., Gallini, R., and Betsholtz, C. (2008) Role of platelet-derived growth factors in physiology and medicine. *Genes Dev. 22*, 1276−1312.

(11) Vincent, L., and Rafii, S. (2004) Vascular frontiers without borders: multifaceted roles of platelet-derived growth factor (PDGF) in supporting postnatal angiogenesis and lymphangiogenesis. *Cancer Cell 6*, 307−309.

(12) Pietras, K., Pahler, J., Bergers, G., and Hanahan, D. (2008) Functions of paracrine PDGF signaling in the proangiogenic tumor stroma revealed by pharmacological targeting. *PLoS Med. 5*, e19.

(13) Jechlinger, M., Sommer, A., Moriggl, R., Seither, P., Kraut, N., Capodiecci, P., Donovan, M., Cordon-Cardo, C., Beug, H., and Grünert, S. (2006) Autocrine PDGFR signaling promotes mammary cancer metastasis. *J. Clin. Invest. 116*, 1561−1570.

(14) Ferrara, N., Hillan, K. J., Gerber, H.-P., and Novotny, W. (2004) Discovery and development of bevacizumab, an anti-VEGF antibody for treating cancer. *Nat. Rev. Drug Discovery 3*, 391−400.

(15) de Vries, C., Escobedo, J. A., Ueno, H., Houck, K., Ferrara, N., and Williams, L. T. (1992) The fms-like tyrosine kinase, a receptor for vascular endothelial growth factor. *Science 255*, 989−991.

(16) Olsson, A.-K., Dimberg, A., Kreuger, J., and Claesson-Welsh, L. (2006) VEGF receptor signalling - in control of vascular function. *Nat. Rev. Mol. Cell Biol. 7*, 359−371.

(17) Shi, W., and Siemann, D. W. (2002) Inhibition of renal cell carcinoma angiogenesis and growth by antisense oligonucleotides targeting vascular endothelial growth factor. *Br. J. Cancer 87*, 119−126.

(18) Madhusudan, S., and Harris, A. L. (2002) Drug inhibition of angiogenesis. *Curr. Opin. Pharmacol. 2*, 403−414.

(19) Manley, P. W., Martiny-Baron, G., Schlaeppi, J.-M., and Wood, J. M. (2002) Therapies directed at vascular endothelial growth factor. *Expert Opin. Investig. Drugs 11*, 1715−1736.

(20) Schenone, S., Bondavalli, F., and Botta, M. (2007) Antiangiogenic agents: an update on small molecule VEGFR inhibitors. *Curr. Med. Chem. 14*, 2495−2516.

(21) Gule, M. K., Chen, Y., Sano, D., Frederick, M. J., Zhou, G., Zhao, M., Milas, Z. L., Galer, C. E., Henderson, Y. C., Jasser, S. A., Schwartz, D. L., Bankson, J. A., Myers, J. N., and Lai, S. Y. (2011) Targeted therapy of VEGFR2 and EGFR significantly inhibits growth of anaplastic thyroid cancer in an orthotopic murine model. *Clin. Cancer Res. 17*, 2281−2291.

(22) McCarty, M. F., Wey, J., Stoeltzing, O., Liu, W., Fan, F., Bucana, C., Mansfield, P. F., Ryan, A. J., and Ellis, L. M. (2004) ZD6474, a vascular endothelial growth factor receptor tyrosine kinase inhibitor with additional activity against epidermal growth factor receptor tyrosine kinase, inhibits orthotopic growth and angiogenesis of gastric cancer. *Mol. Cancer Ther. 3*, 1041−1048.

(23) Wedge, S. R., Ogilvie, D. J., Dukes, M., Kendrew, J., Chester, R., Jackson, J. A., Boffey, S. J., Valentine, P. J., Curwen, J. O., Musgrove, H. L., Graham, G. A., Hughes, G. D., Thomas, A. P., Stokes, E. S. E., Curry, B., Richmond, G. H. P., Wadsworth, P. F., Bigley, A. L., and Hennequin, L. F. (2002) ZD6474 inhibits vascular endothelial growth factor signaling, angiogenesis, and tumor growth following oral administration. *Cancer Res. 62*, 4645−4655.

(24) Taguchi, F., Koh, Y., Koizumi, F., Tamura, T., Saijo, N., and Nishio, K. (2004) Anticancer effects of ZD6474, a VEGF receptor tyrosine kinase inhibitor, in gefitinib ("Iressa")-sensitive and resistant xenograft models. *Cancer Sci. 95*, 984−989.

(25) Ryan, A. J., and Wedge, S. R. (2005) ZD6474−a novel inhibitor of VEGFR and EGFR tyrosine kinase activity. *Br. J. Cancer 92* (Suppl 1), S6−13.

(26) Drevs, J., Konerding, M. A., Wolloscheck, T., Wedge, S. R., Ryan, A. J., Ogilvie, D. J., and Esser, N. (2004) The VEGF receptor tyrosine kinase inhibitor, ZD6474, inhibits angiogenesis and affects microvascular architecture within an orthotopically implanted renal cell carcinoma. *Angiogenesis 7*, 347−354.

(27) Matsumori, Y., Yano, S., Goto, H., Nakataki, E., Wedge, S. R., Ryan, A. J., and Sone, S. (2006) ZD6474, an inhibitor of vascular endothelial growth factor receptor tyrosine kinase, inhibits growth of experimental lung metastasis and production of malignant pleural effusions in a non-small cell lung cancer model. *Oncol. Res. 16*, 15−26.

(28) Commander, H., Whiteside, G., and Perry, C. (2011) Vandetanib: first global approval. *Drugs 71*, 1355−1365.

(29) Park, K., Kim, Y.-S., Lee, G. Y., Nam, J.-O., Lee, S. K., Park, R.-W., Kim, S. Y., Kim, I.-S., and Byun, Y. (2007) Antiangiogenic effect of bile acid acylated heparin derivative. *Pharm. Res. 24*, 176−185.